The Earth's Radiation Belts

Belts of charged particles surrounding the earth were a surprising discovery of the early artificial satellites. In eight years much has been learned about their geometry and injection and loss mechanisms, but many questions remain.

by R. Stephen White

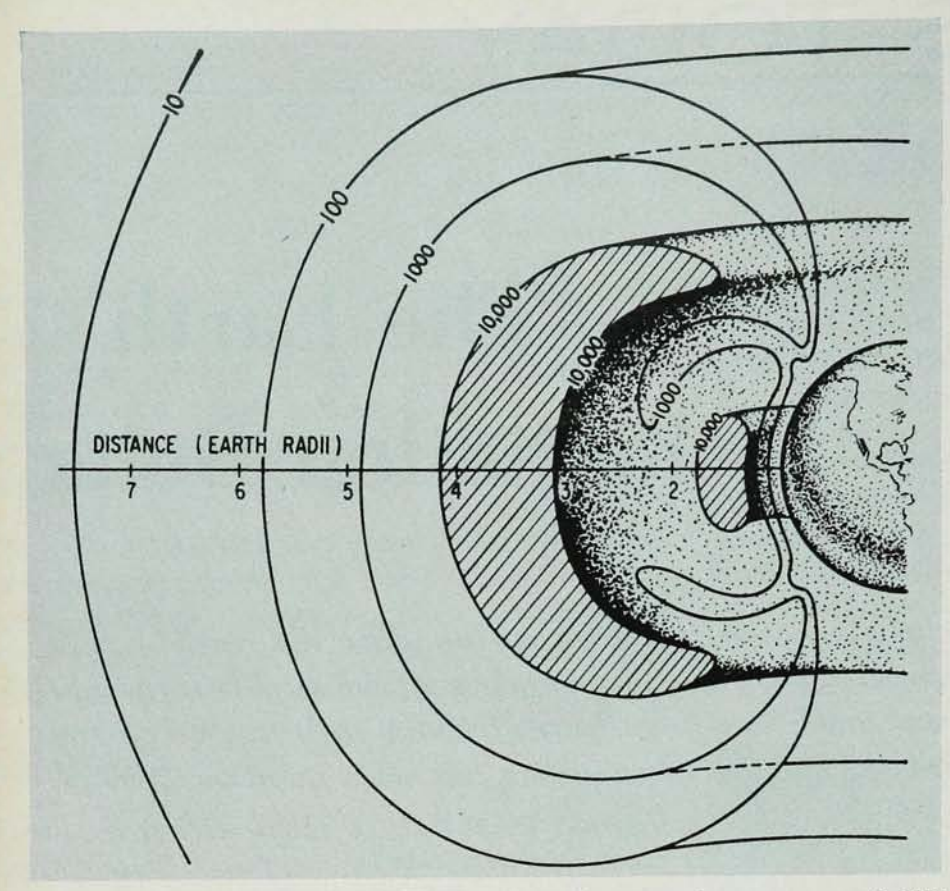
EIGHT YEARS of space experimentation have elapsed since James A. Van Allen, George H. Ludwig, Carl E. McIlwain and E. C. Ray¹ discovered the earth's radiation belts with a Geiger counter on the Explorer 1 satellite. Almost every flight since has offered the opportunity of finding a different particle, a new energy distribution or an unusual space or time variation.

At first there were only two belts, an inner and an outer belt. The inner belt was centered at an altitude of 3000 km. The outer belt, with a maximum at about 25 000 km, was added with the discovery of a second large radiation zone by a Geiger counter on the moon probe Pioneer 3.2 These belts were beautifully displayed in a review article by Van Allen3 in 1959 and are reproduced here in figure 1.

The shapes of the inner and outer electron belts, in three dimensions, are sketched in figure 2 with the three types of charged-particle motion superimposed. The particle circles the magnetic field line with the familiar cyclo-

tron motion, bounces back and forth along the magnetic field line and drifts around the earth on a magnetic L shell; the electrons drift east and the protons west. L is the distance to the magnetic shell at the equator, usually given in earth radii. Each L shell is formed by rotating a magnetic field line about the earth's magnetic dipole axis. Slight changes from this shape arise because of the deviations of the true magnetic field from a dipole field. Since the particle always mirrors at the same value of B as it drifts around on its L shell, its motion can be described by the L shell on which it

R. Stephen White received a PhD in physics from the University of California in 1951. For several years thereafter, he taught physics at the university and worked in the Lawrence Radiation Laboratory. Since 1961 he has been head of the Particles and Fields Department of the Space Physics Laboratory of the Aerospace Corporation at Los Angeles.



INNER AND OUTER RADIATION BELTS taken from Van Allen,³ 1959. The belts are indicated by the slanted

lines. Contours of count rates of 1000, 100, and 10 are also indicated. Distances in earth radii are labeled. -FIG. 1

Definitions of Symbols

B earth's magnetic field (gauss).

C a constant.

dE/dx the ionization energy loss per unit path length in the atmosphere, proportional to ρ .

ds distance along the magnetic field line.

E the particle kinetic energy.

the particle kinetic energy associated with the velocity perpendicular to B.

J second adiabatic invariant.

 flux of particles (number/cm²-secster-MeV).

id flux of daughter electrons.

im flux of parent electrons.

in flux of albedo neutrons at the position of injection.

in flux of trapped protons.

L magnetic shell coordinate, the distance to the magnetic shell at the equator $(r_{\rm e})$.

M magnetic moment of the earth.

p_{II} momentum parallel to the magnetic

R radial distance from the center of the earth.

re radius of the earth.

v velocity of the albedo neutron, also

of the decay proton because it carries away almost all of the neutron momentum.

angle between the particle velocity and magnetic field directions at the equator.

$$\left[1 - \left(\frac{v}{c}\right)^2\right]^{-\frac{1}{2}}$$
. c is the velocity

of light.

mean atmospheric density averaged over the particle's trajectory in the earth's magnetic field.

latitude.

Ta

 τ_{m}

mean lifetime.

mean lifetime of daughter electrons. mean lifetime of parent electrons. magnetic moment, first adiabatic in-

variant

injection coefficient, the probability
that the proton from the albedo
neutron decay makes a sufficiently
large angle with the magnetic field
direction that the proton is initially
trapped.

moves and the B value at which it mirrors.

High-energy protons

The Geiger counter is an excellent exploratory detector and has been used with great success by Van Allen and coworkers. But it was not able to identify the particles in the radiation belts.

Early in 1959, Stanley C. Freden and I⁴ had the opportunity of flying small stacks of nuclear emulsions on Air Force missile nose cones. These were recovered down range from Cape Kennedy after reaching an altitude of 1200 km. With emulsions it was possible to distinguish among protons, alpha particles and electrons and even deuterons, tritons and ³He particles.

The first successful recovery of a Thor nose cone in April 1959 gave excellent results. The emulsions were loaded with proton tracks. Shielding around the emulsions stopped protons of less than 75 MeV and electrons of less than 12 MeV. (No electrons were seen.) That first proton energy distribution is shown in figure 3. Subsequent flights in May 1959 and October 19605, 6 pushed the proton energy distribution down to 10 MeV. No electrons above 5 MeV were observed. The number of deuterons and tritons was only 1% of the number of protons. No alpha particles were detected. This was not surprising since the minimum detectable energy for alpha particles was very high-300 MeV.

The explanation for the trapped in protons first came from S. Fred Singer.7 He recognized that cosmic-ray protons collide with atmospheric nuclei and that the product neutrons stream back into the magnetosphere and decay into protons, electrons and neutrinos. The charged electrons and protons spiral around the magnetic field lines and move around the earth trapped on magnetic shells. The protons lose energy by ionization and excitation of atmospheric atoms, and an equilibrium distribution is then maintained between the cosmic-ray albedo neutrondecay source (CRAND) and the atmospheric sink. Singer predicted the shape of the proton energy distribution. Later another loss mechanism, nuclear interactions,5 was added to the theory. This is significant for protons above 75 MeV. The CRAND injection into the highenergy proton belt is shown in figure 4.

At equilibrium, the number of protons injected (protons/cm³-sec-MeV) must equal the number lost. Consider the simplest case: trapped protons of less than 100 MeV with ionization loss only. Take power laws in energy for the neutron albedo flux j_n , the ionization energy loss dE/dx, the trapped proton flux j_p , the proton velocity v, and γ (defined in the list on page 26). Then the equilibrium proton flux is

$$j_p = \frac{C \ \chi \ j_n (E) E^{1.28}}{\rho}$$
 (1)

We see that j_p is proportional to the injection coefficient χ and to j_n and is inversely proportional to the mean atmospheric density averaged over the particle trajectory ρ . C is a constant. Before the theoretical expected equilibrium flux can be determined, χ , ρ and j_n must be evaluated.

The early calculations took χ equal to one, a big overestimate. Recently, computations⁸ that simulate the ejection of neutrons from the earth have been made with a computer program. Various neutron latitude and zenith angle distributions were used. χ varies somewhat with these distributions and with position in space but on the average is about 0.1 for the CRAND source.

Trapped protons can also be injected from solar proton albedo neutron decays (spand). Solar protons arise from solar flares. The computed χ for spand injection is even lower than for crand because neutrons from the poles are less likely to inject trapped protons than neutrons from the equator. The uncertainties in the χ 's for the cases considered, are much less than 50% since the calculations are strictly geometric.

The ρ is obtained by averaging the atmospheric density over a proton drift period around the earth. A model atmosphere and a magnetic-field representation are required for the computation. At a few hundred kilometers, near the lower edge of the trapped-radiation belt, the atmospheric densities are known from satellite drag measurements to better than a factor of two. However, the densities change rapidly with altitude. The exponentially decreasing distance is approximately 50 km, so the proton trajectmately

tories through this atmosphere must be precisely known. The currently used 48- and 512-term representations of the earth's magnetic field give differences as large as a factor of 10 in the mean densities. Above 1000-km altitudes the magnetic-field differences are of less importance, but the atmospheric densities are less well known. Local atmospheric anomalies or changes with latitude and longitude have not been well investigated. The uncertainty in j_p due to ρ in some regions of space can be as large as a factor of 10.

Singer⁷ estimated the albedo neutron flux from the proton reaction fragments of cosmic-ray proton interactions in nuclear emulsions. Wilmot N. Hess,¹⁰ on the other hand, used the neutron flux below 10 MeV, measured in the atmosphere at airplane altitudes with BF₃ counters, and connected this to the cosmic-ray spectrum at 1 BeV. The input neutron spectrum between 10 and 100 MeV is necessary for comparison between experiment and theory but is currently the most poorly known part of the theory.⁸ A factor-of-10 uncertainty in the albedo neutron flux is realistic.

Late in 1959, on Explorer 6, C. Y. Fan, P. Meyer and J. Arol Simpson¹¹ found that the protons decreased rapidly at distances greater than 4000 km above the surface of the earth. This decrease could not be explained by the CRAND source, since CRAND injection should only vary slowly in that region of space. Singer¹² suggested that this effect came from breakdown of the first adiabatic invariant, the magnetic moment

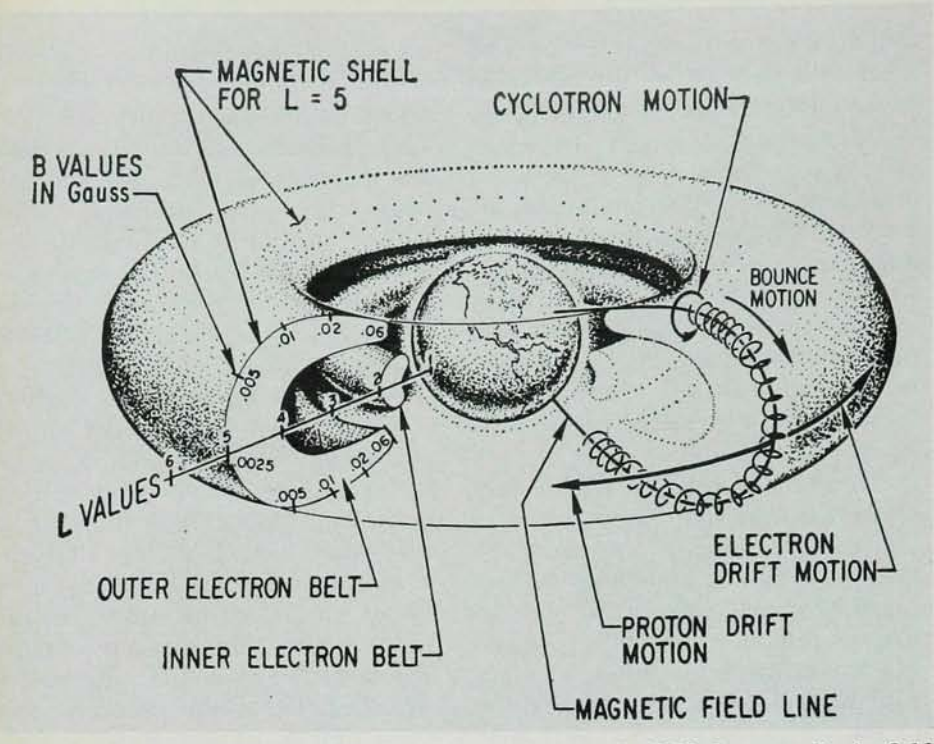
$$\mu = E_{\perp}/B \tag{2}$$

E, is the proton energy associated with the velocity perpendicular to the magnetic field B. At large distances from the earth, time or space variations in B can be as large as the steady magnetic field. If these variations occur in times or regions of space that are small compared to the proton cyclotron period or radius, μ invariance is violated. The protons are then driven down into the denser atmosphere where they are quickly lost. Alex J. Dragt13 suggested that hydromagnetic waves are responsible for the breakdown. He calculated the losses and found them of reasonable size to account for the low proton

fluxes at great distances from the earth. Consequently an additional term representing diffusion in pitch angle (the angle between the proton direction and the magnetic field) caused by electromagnetic wave interactions should be added to the equilibrium equation for the trapped proton flux. It is hoped that the predicted hydromagnetic waves at a frequency of about 1 Hz will soon be observed in space.

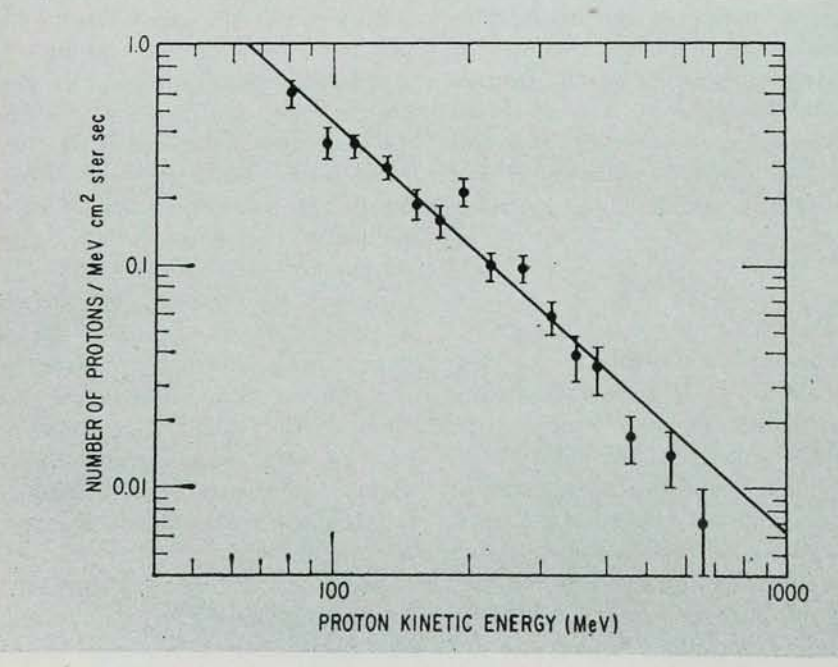
John E. Naugle and D. A. Kniffen¹⁴ obtained energy distributions of protons with nuclear emulsions at a number of altitudes on the probe NERV in September 1960. These distributions were of particular interest because they showed that protons with energies of 10 MeV increased in number rapidly with altitude. These protons were first observed to increase at the altitude and space location where neutrons could decay after straight-line travel from the earth's polar cap. Since the earth's polar cap is bombarded by protons from the sun at times of solar flares and the solar flare proton energy distribution is much softer than the cosmic ray primary spectrum, the SPAND injection was considered a prime candidate for the source of the low-energy protons. Allen M. Lenchek15 computed the flux and energy distribution to be expected and concluded that SPAND was indeed a likely source. There should be no spand-injected protons for L < 1.5 and there should be no spandinjected protons at higher L values at the equator. Neither of these predictions seems to be verified by later measurements with scintillators and solid-state detectors.16, 17, 18 The abrupt increase of the flux at L = 1.5 suggested by the emulsion measurements is not found. In addition, the lowenergy protons are more abundant at the equator than at higher B values close to the earth. The discrepancy between the experiments and the theory and between the emulsion and the counter measurements has not yet been resolved.

Although the energy distributions measured with nuclear emulsions are still the most detailed, they have one serious drawback. Nuclear emulsions must be recovered before the data can be analyzed. For that reason they are not useful for extended spatial distributions. The spatial measurements



THE TWO ELECTRON RADIATION BELTS. They appear horseshoe shaped in the cutaway. The cyclotron motion about the magnetic field line, the bounce motion along the line, and the drift motion around the earth are shown. Protons drift westward, electrons eastward. A magnetic L shell is formed by rotating a magnetic field line about the earth's magnetic dipole axis. The deviations of the

true magnetic field from a dipole field change the shape slightly. L is the distance to the shell in earth radii. Each particle always mirrors at its same value of B. The particle motion is thus described by the L shell on which it moves and the B value at which it mirrors. The magnetic shell for L=5 is labeled. B values in gauss are noted. L values on a radial line are indicated. -FIG. 2



TRAPPED PROTON ENERGY DISTRI-BUTION as measured by Freden and White,⁴ 1959. The shape of this distribution and subsequent ones^{5,6} were well fit by cosmic ray albedo neutron decay injection and atmospheric ionization and nuclear collision losses. Recent calculations⁵ show that this theory will give enough trapped protons only if the ratio of neutron albedo flux to the atmospheric density is a factor of 50 larger than is currently estimated.

—FIG. 3

have been obtained with counters that read out directly into telemetry over a receiving station or onto a tape recorder that is played into telemetry when the satellite passes over a receiving station.

The constraints forced upon space experiments are usually quite severe. The experiments must be lightweight, typically 2 to 10 kg, and must draw low power, typically 1 W. Telemetry is seldom as much as desired. No multiton magnets or large shielding blocks like those considered essential around accelerators are permitted. After launch of the experiments no discriminators can be tweeked or circuits repaired. It is not possible to stop, redesign the experiment and try again at a later date. For these reasons identification of radiation-belt particles and measurements of their fluxes and energies have proceeded slower than measurements on the ground.

In addition to instrumentation difficulties, are the difficulties that the trapped radiation belts are not constant in space and in much of space are not constant in time. One nice simplification to the data handling has been added by McIlwain. The three space coördinates, latitude, longitude and altitude, are replaced by just two: B and L. L is a function of B and of the second adiabatic invariant J, defined as 20

$$J = \oint p_{\mathbf{n}} ds \tag{3}$$

 (p_{\parallel}) is the momentum parallel to the magnetic field and ds is measured along the line). The line integral is taken over one complete bounce motion from one mirror point to its conjugate and back again.

Plastic scintillators¹⁶ with fixed thresholds show that the proton energy distributions vary greatly with position in space. The two peaks found in the curve of flux as a function of L for protons with energies of 40 to 110 MeV are shown in figure 5. The outer peak was found at L=2.2 and the inner peak as before at L=1.5. Neither crand nor spand explains the double peaks. If higher-energy protons had been plotted, the L=1.5 peak would have been closer in. And the peak for lower-energy protons would have been farther out.

Additional energy distributions and

fluxes as a function of B and L have been measured with plastic and solidstate detectors17, 18 and with emulsions.21 These measured distributions are not explained either. In fact, recent CRAND calculations8 of the fluxes are too low by a factor of 50 to explain the trapped protons at low altitudes and spand is an additional factor of 10 lower. A possible explanation is that the ratio of the currently accepted albedo neutron flux to the mean atmospheric density encountered by the trapped protons used in the calculations is a factor of 50 too low. A measurement of the earth's albedo neutron energy distribution in the energy range of 10 to 100 MeV is badly needed.

It is likely that another source is responsible for protons with energies less than 10 MeV. This leads us to the low energy proton distributions and the inward diffusion source.

Low-energy protons

The low-energy proton belts surround the earth in multilayers like concentric onion skins. The lowest-energy protons are on the outside and the higher-energy ones are closer in. Three of the proton belts are shown in figure 6 at L=4.5, 3.5, and 2.5. The belts are shown as separated, but they run continuously from one energy to the next.

Intense fluxes of these low-energy protons were discovered by Leo R. Davis and James M. Williamson²² on Explorer 12, which was launched in August 1961. They found 6 × 107 protons/cm2-sec-ster on the equator at L = 3.5 with E > 0.1 MeV. Integral energy distributions, measured from 0.1 to 1.6 MeV, became harder at lower L values. Davis and Williamson obtained additional measurements from Explorers 14 and 15. The energy distribution from 1 to 10 MeV was measured by S. J. Bame and his coworkers23 on a rocket launched in October 1960, which went along a magnetic field line at L=2.

Paul J. Kellogg²⁺ had pointed out in 1959 that particles diffusing inward at the equator while conserving the first adiabatic invariant should increase their energies E according to

$$EL^3 = \text{const}$$
 (4)

Equation 4 is obtained by substituting the expression for a magnetic dipole

field, $B = M/L^3$, into equation 2. M stands for the magnetic moment of the earth.

In 1960 E. N. Parker²⁵ invented a mechanism for obtaining the diffusion. The third adiabatic invariant, which is the total magnetic flux through the drift orbit, is violated. Sudden impulses in the magnetic field, which come in a time short compared to the drift period of the protons, cause betatron acceleration in the drift orbit. The drift period is inversely proportional to E and Land is about 15 minutes. The acceleration is about 10 keV for a large storm. The orbits are pushed inward for some protons and outward for others. Relaxation back to the original condition occurs adiabatically. This causes a random walk in L. Parker found a diffusion constant that increased outward as L^{10} . These ideas were applied 26 to calculate the constant in the exponential of the proton integral energy distribution. It was found to increase toward higher L values in agreement with the measured value.

M. Paul Nakada and G. D. Mead²⁷ used a Fokker-Planck diffusion equation to obtain the theoretical proton spatial and energy distributions along the equator. They included diffusion coefficients for the mean value of the displacement in R and R^2 , proportional to L^9 and L^{10} , respectively, an exponential integral energy distribution at the edge of the magnetosphere, and Coulomb-energy and charge-exchange losses.

The theory can be compared to the recent data of John D. Mihalov and me.28 We measured the differential spatial and energy distributions of protons at 12 energies between 0.2 and 6 MeV with a cesium-iodide spectrometer on the satellite 1964-45A. We found that at the lowest measured energy-0.19 MeV-the population has its maximum value at L = 4.5 while at the highest energy-2.8 MeV-it has its maximum at L = 2.4. These maxima appear to be independent of B and so can be applied to the equator. The values of EL3 indicate that the first invariant is conserved up to an energy of 0.75 MeV but not at higher energies. Off the equator, $EL^3 \sin^2 \alpha_0(L)$ should be constant if both the first and second adiabatic invariants are conserved. The pitch angle at the equator, $\alpha_0(L)$, is evaluated along a drift trajectory. Since the experimental $EL^3 \sin^2 \alpha_0(L)$ deviates even more from a constant than EL^3 we also conclude that the first and second invariants are not conserved for energies above 0.75 MeV.

The theoretical spatial and energy distributions²⁷ were derived for positions on the equator only and were not extended to the B values of our experiment.²⁸ Nevertheless, the general features of the theory do not appear to depend strongly on this fact; so the theory is compared to the experimental data at B=0.10 G. These general features are in good agreement with the experimental ones. The detailed comparisons of the spatial distributions, however, show some important differences.

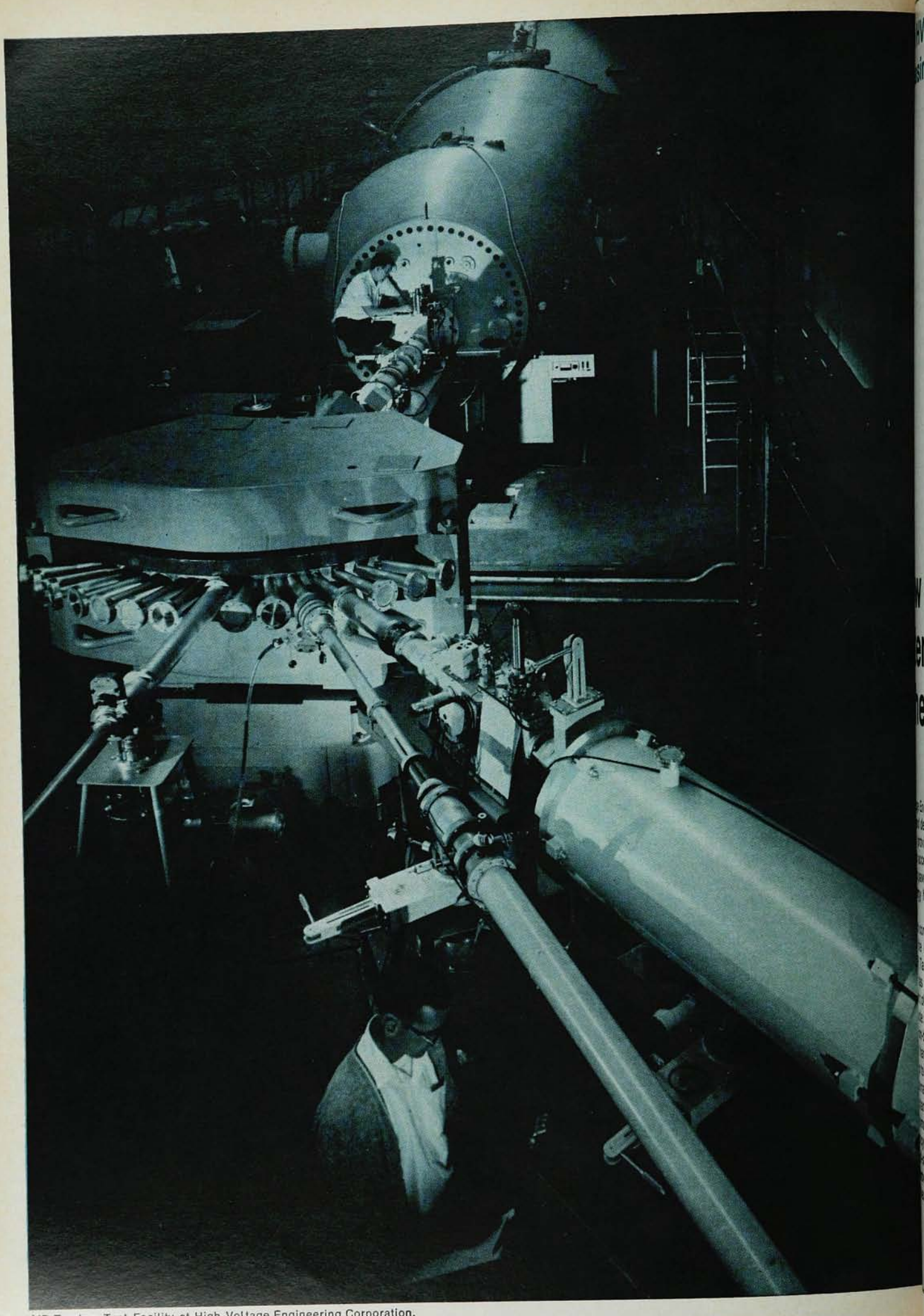
The experimental energy distributions²⁸ of figure 7 have narrow peaks. Indeed, the true energy peak widths must be very narrow because the observed widths are comparable to the energy resolutions. If these protons are due to diffusion inward, a peaked proton source of 15 keV at L=10 at the edge of the magnetosphere is required. In the theoretical energy distributions the turnover at low energies is caused by the proton losses, however, and not by the source since an exponential energy source at L=10 at the edge of the magnetosphere was assumed.

At low L values, the theoretical distributions are too low at low energies; that is, at L=2.0 and E=0.40 MeV the theoretical value is a factor of 100 lower than the experimental value. The agreement between theory and experiment would be improved by using a larger diffusion rate.

At low L values diffusion is so slow and the proton losses so great that the fluxes fall extremely rapidly between L=3.25 and L=2.35. For L<2.0, it seems very difficult to account for the protons by diffusion inward from the magnetospheric boundary.

It is interesting that the straight-line power-law fits to the energy distributions of figure 7 are also in reasonable agreement with the data at 55 MeV.¹⁷ This agreement is over an energy range of a factor of 100 and a flux range of 2×10^{7} .

Finally, we should emphasize that the diffusion theories have not calculated the absolute number of protons injected into the earth's magnetic field. Consequently a prediction of the abso-



MP Tandem Test Facility at High Voltage Engineering Corporation.

From HVEC's research program for increasing tandem accelerator flexibility:

New developments extend research capabilities of heavy-ion accelerators.

High Voltage Engineering's expanded assearch and development efforts are geared to provide greater flexibility or present accelerator research programs, and pave the way for the new, igher-energy heavy-ion tandems of the future.

Research conducted this past summer with the company's new 'Emperor' (MP) Tandem Accelerator, for example, has concentrated on the development of several new concepts. These include:

A new ion-beam injector system, capable of handling a wide range of elements up to and including uranium.

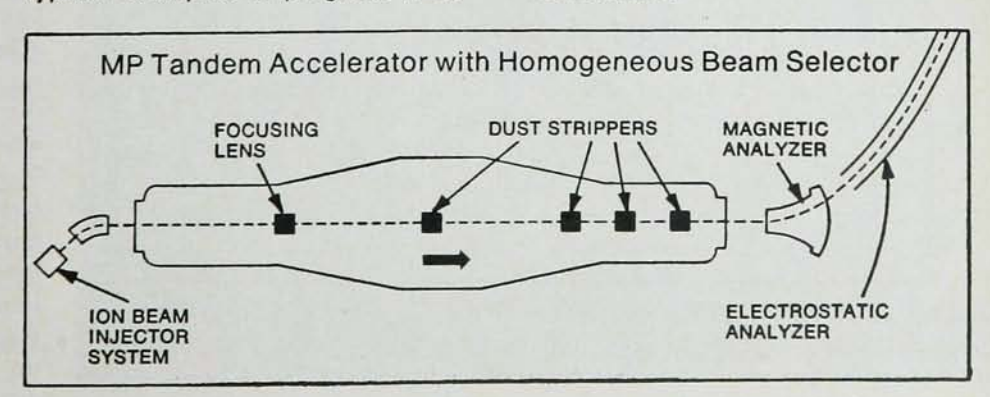
New internal focusing lenses designed to channel and direct charged particle beams with greater precision and efficiency.

Newsolid-state "dust" strippers caable of providing significant quanlies of heavy ions at energies higher than ever before possible.

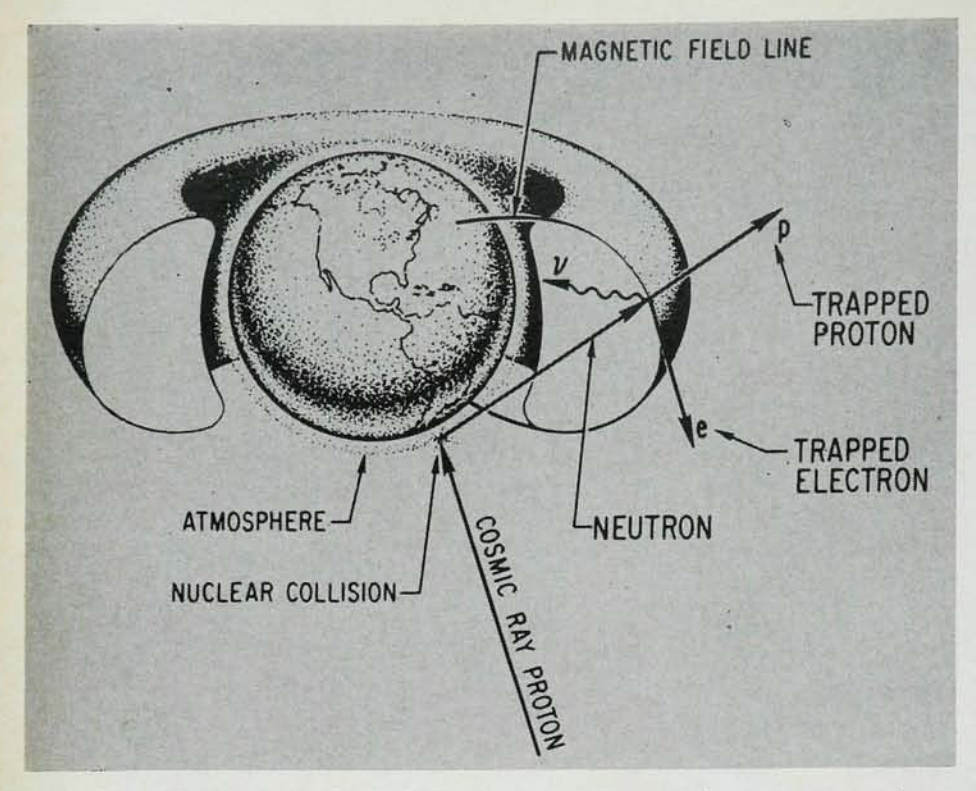
A new beam-analyzing system, composed of magnetic and electrostatic components to provide researchers with a homogeneous beam of ions of known mass, energy, and charge.

New developments like these are typical examples of progress in accelerator capabilities from HVEC, recognized leader in particle accelerator and related technologies. For additional information and technical literature on tandem accelerators write to:

High Voltage Engineering Corporation, Burlington, Massachusetts, 01803 (Tel: 617-272-2800) or Amersfoort, The Netherlands.



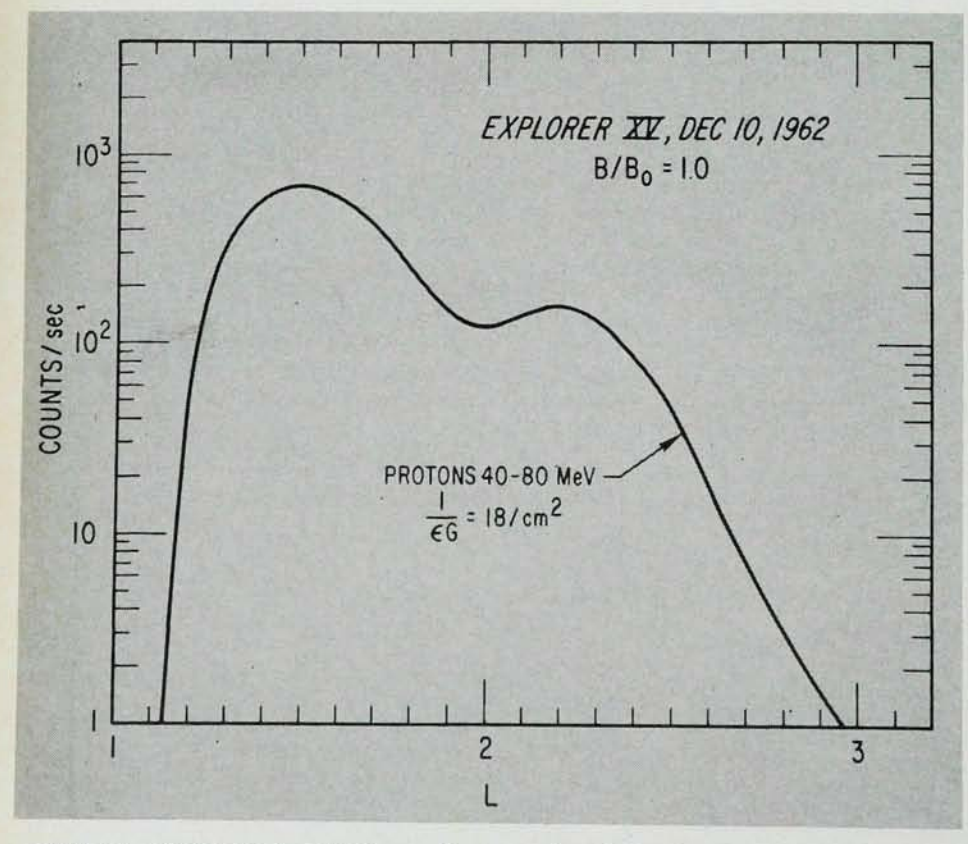




THE HIGH-ENERGY PROTON BELT. Actually the proton belts are displaced for different energies. 75-MeV protons peak at L=1.5 but lower-energy protons peak farther out. The cosmic-ray albedoneutron decay injection, CRAND, is

shown. The cosmic-ray proton makes a nuclear collision in the atmosphere and emits a neutron. The neutron decays into a proton, electron, and neutrino. The electron and proton are trapped in the earth's magnetic field.

-FIG. 4



PROTON COUNTING RATE at the equator for 40-110-MeV protons taken from McIlwain, 16 1963. This shows two

maxima. The first is at L=1.5 and the second is at L=2.2. Data taken at the equator, $B/B_0=1.0$.

lute number of trapped low-energy protons has not been made. Until the injection mechanism is known and absolute equilibrium fluxes can be calculated, the explanation for these protons is inadequate.

Electrons

Today there are two great electron belts—the inner belt and the outer belt. These are shown in figures 1 and 2. The inner belt consists mostly of the fission-electron remains of Starfish, the United States high-altitude nuclear burst, which was exploded in July 1962. This belt is now peaked at L=1.35. These electrons do not fluctuate, only slowly decrease with time.

The outer belt is peaked at L=5 and is separated from the inner belt by a large slot. It is made up of natural electrons of lower energy. It varies considerably with time and is correlated with changes in the magnetic field. How the electrons got there is still an unanswered question.

Extensive surveys have been carried out by Van Allen and his coworkers. They have measured the spatial distributions of particles in great detail on Explorers 1, 4, 7, 12, and 14^{1, 2, 29, 30, 31, 32} and have found that the flux of electrons with energies greater than 40 keV in the outer belt in September 1961 was 10⁸ electrons/cm²-sec.²⁹ Since then there have been large time variations, but the flux is usually within a factor of 10 of 10⁷ electrons/cm²-sec. The average value has been rather constant over the last 6 years.

Lity

E DEE

100

Man

Min

the

TOTAL

Side !

S. G

d for t

地

appl

N 200

Phops

Mediani O Alectro

Kibm

Starf

物

K. I. Gringauz and coworkers33 discovered fluxes of 107 electrons/cm2-sec with energies greater than 200 eV with a Faraday Cup on Lunik 2 at 50 000 to 80 000 km from the earth in a backward direction of 45 deg to the sun-earth line. They34 also observed the low-energy electrons with Lunik l, which had a trajectory tilted at about 75 deg to the sun-earth direction. They considered the electrons as a third or outermost belt. These electrons are now thought to be part of the magnetosphere tail or transition region (see below, "Magnetic cavity"). Also on Lunik 2,35 approximately 5 × 105 electrons/cm2-sec were found with energies between 1 and 2 MeV. These measurements suggested that the previous Geiger-counter measurements^{2,11} were really due to penetrating electrons and not to bremsstrahlung as had been supposed.

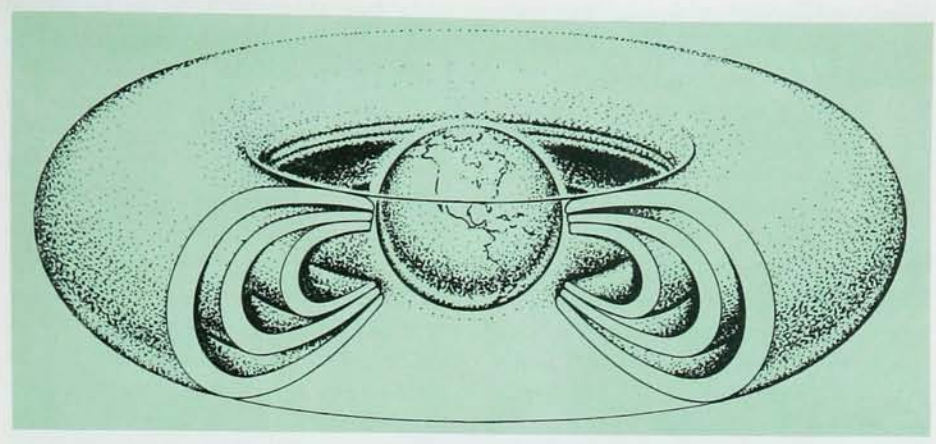
No reliable measurements were made of the electron fluxes at the equator at the maximum of the inner radiation belt before July 1962. However, the natural electrons of the inner radiation belt were identified, and their energies were measured³⁶ by Atlas pods at altitudes of 1500 km in 1959. The differential energy spectrum measured at $L \approx 1.3$, $B \approx 0.25$ decreased by a factor of 20 from 100 to 450 keV.

The electrons of the outer belt were identified, and their energies measured on Javelin rockets.³⁷ Between 50 and 700 keV, an exponential energy distribution with an *e*-folding energy of 60 keV was found. This was considerably steeper than the one in the inner radiation belt.

Calculations were made by Hess and his colleagues³⁸ using CRAND injection and atmospheric energy loss and scattering. They concluded that one could explain the electrons on the basis of CRAND injection if the electron lifetimes at the equator were longer than about 10 years. They also computed the theoretical energy distributions but found them flatter than the measured ones. Relatively more electrons were found experimentally at low altitudes than predicted by the neutron-decay theory.³⁹

The outer-belt electron fluxes were found experimentally to increase and then return to normal in times as short as a month.³⁰ Measurements by B. J. O'Brien⁴⁰ of large fluxes of electrons with small pitch angles indicate that such large fluxes of electrons are continuously lost into the atmosphere and that the lifetimes have to be short. Therefore, CRAND injection seems impossible for the outer radiation belt. And the slot between the two belts has not been explained.

Before more sophisticated measurements could clarify the injection and loss mechanisms, Starfish injected enough electrons into the inner radiation belt to mask the natural electrons entirely. Starfish exploded at an altitude of 400 km on 6 July 1962 over Johnson Island in the Pacific. The yield was 2 megatons, and 2 × 10⁸ fission electrons/cm²-sec were injected



THREE LOW-ENERGY PROTON BELTS at L=4.5, 3.5 and 2.5. The belts overlap so that there are no gaps. The lowest energy protons peak at high L

values and higher energy protons peak closer in. These belts probably originate from diffusion inward from the solar wind across field lines. —FIG. 6

at the maximum of the inner radiation belt at L=1.3. Shortly thereafter, the Russians followed with three nuclear injections on 22 and 28 Oct. and 1 Nov. at L values of 1.88, 1.81 and 1.77.^{41, 42}

These were not the first nuclear explosions in space. Following the suggestion of Nicholas Christofilos⁴³ in an unpublished memorandum in 1957 that many geophysical effects could be observed, three nuclear explosions, called Argus, were carried out by the Advanced Research Projects Agency. The 1- to 2-kiloton bursts occurred on 27 and 30 Aug. and 6 Sept. 1958 at 480 km over the South Atlantic. Experiments44 on Explorer 4 found that the drift in latitude of the Argus III shell at L = 2.2 was less than 0.03 deg latitude/day or less than 1 km/day radially. They found that the count rate fell off as 1/t for the first 10 days.

Since the electrons were injected into the radiation belts at known times, it was possible to follow the electron fluxes as a function of time and to measure the lifetimes of the electrons. Lifetimes for the Russian electrons were measured to be only a few days. 16, 30, 41, 42, 45 Lifetimes for Starfish electrons initially were just as short but quickly increased to about one year.46, 47, 48 These lifetimes are summarized in the table. The lifetime48 as a function of L is given in figure 8. Martin Walt+9 calculated the expected lifetimes using a Fokker-Planck diffusion equation and losses by scattering and ionization in the atmosphere. These agreed very well with the experimental decay curves from a few hours up to 50 days for 0.18 < B < 0.22 G for $L \le 1.3$, which indicated that the atmosphere controls the lifetimes there. But for L > 1.3 the calculated lifetimes were longer than the experimentally measured values.

At a particular position in *B-L* space, electrons that were injected initially are augmented with those from lower *B* values (higher altitudes) by scattering. Electrons are lost by the same process. Atmospheric density decreases rapidly as *B* decreases (the altitude increases). Transient equilibrium is established between the electrons at high and low altitudes. The problem is similar to that of radioactive decay where the parent-daughter relationship gives the flux of the daughter proportional to the parent as

$$j_{\rm d} = \frac{j_{\rm m}}{\tau_{\rm m}} \, \tau_{\rm d} \tag{5}$$

j is the flux of electrons/cm²-sec, τ is the mean lifetime in seconds, m signifies the parent and d the daughter. The $j_{\rm d}$ decreases at the same rate as the $j_{\rm m}$ which falls off exponentially with a lifetime of $\tau_{\rm m}$. From the table it can be seen that transient equilibrium was reached rather rapidly in most parts of space. The maximum lifetime is measured at the equator at L=1.5 and is about 2 years. Higher and lower L values give shorter lifetimes. If the atmosphere and electron trajectories in the earth's magnetic field are not greatly different from

those used by Walt,⁴⁹ another nonatmospheric loss mechanism must become important for electrons for L > 1.3.

Detailed electron energy distributions were measured at five energies in a 180-deg focusing magnetic spectrometer. The measurements were made on the satellite 1962 β K (STARAD), which was launched on 26 Oct. 1962. They showed that the Starfish electrons had fission energy distributions. The electron spectra of the Russian injections were similar. For higher L, the energy distributions at selected B and L values are given in figure 9.

At low altitudes William L. Imhof and R. V. Smith⁵⁰ observed an unexpected narrow peak at 1.3 MeV, L=1.15 and B=0.217, which decayed away with a time constant of one day. The time constant is just that expected from atmospheric losses. This decay can be explained by time oscillations in the earth's magnetic field.⁵¹ These oscillations are in resonance with the drift period of specific-energy electrons, which diffuse to lower L values. Nearly monoenergetic electrons then appear at positions in space where none previously existed.

After the Starfish and the Russian injections the slot was temporarily filled but rapidly emptied again to separate the inner from the outer radiation belt. Walter L. Brown and J. D. Gabbe⁴⁶ reported a time constant of 5 days for $2.2 \le L \le 3.0$. There must be large electron losses in this region of space. If the losses are atmospheric only, a large peak in the atmospheric density contour between L=2 and L=3 is required. Such a peak has not been identified. The only latitude effect appearing in present atmospheric models is the sun's diurnal variation.

100

14

120

370

N di

		Measurement			Electron				
I	njection	L (earth radii) 2.0 2.2 2.5	B (gauss) 0.04-0.08 0.05-0.10 0.06-0.14	Measurement date 20 July 1962	energy (MeV)	Mean lifetime (days) 15 4 5		Authors Brown and Gabbe ⁴⁶	
Starfish,	6 July 1962								
		3.0 3.5	0.07-0.17 0.10-0.20			4 14			
		1.5	0.094	10 Dec. 1962	>0.5			McIlwain ¹⁶	
		2.0	0.40			50			
		1.5 2.0	0.94 0.40		>5.0	50 50			
		1.2	0.185	1963	>0.5	140		McIlwain—Reported in Walt4	
		1.3	0.146			270			
		1.4 1.5	0.119 0.094			270 270			
		1.20 1.23 1.30 1.40	0.185-0.205 0.170-0.205 0.160-0.230 0.165-0.210	22 Dec. 1963	>1.2	120±12 165±50 235±20 390±40	130±20 190±30 320±70 500±100	Bostrom and Williams ⁴⁷	Van Allen ⁴⁸
		1.50 1.60	0.175-0.215 0.180-0.225			460±50 360±50	590±300		
Russian	22 Oct. 1962 28 Oct 1962	2.8	0.017-0.038	28 Oct. 1962– 14 Feb. 1963	>1.6	30		Frank, Van Allen, Hills ³⁰	
	22 Oct. 1962 28 Oct. 1962 1 Nov. 1962	2.80-3.10	0.330-0.355	10-30 Nov. 1962 10-30 Dec. 1962	>3.9	20 50		Burrows and McDiarmid ⁴¹ *	
	1 Nov. 1962	1.77	0.252	6–10 Nov. 1962	0.35 bremsstrahlung	7 +4 -2		Mihalov, Mozer and White ⁴²	

^{*}Burrows and McDiarmid fit their decay data to a power series in time $I = I_o t$ - η . Over a period of 2 months following the 3 injections $\eta \approx 1.3$ at L = 2.05, B = 0.240; L = 2.20, B = 0.250, L = 2.55, B = 0.260; and L = 2.95, B = 0.270. The values appearing in the table are exponential approximations at the times indicated.

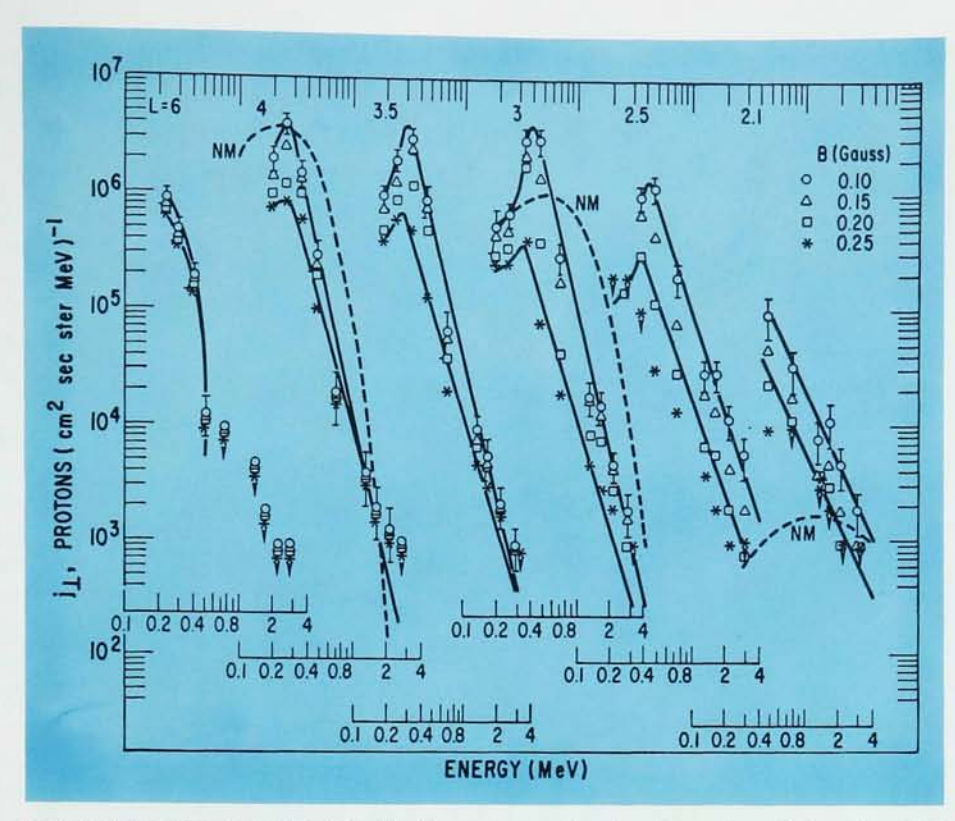
In the fall of 1962, on low altitude polar satellites, George A. Paulikas and Freden⁵² observed semitrapped fluxes of 10^3 electrons/cm²-sec with energies greater than 0.9 MeV at L=1.2 and L=2.0. These electrons were lost when they dipped deep into the atmosphere in their drift trajectories over the South Atlantic. They probably leaked out of the Starfish belt. Perhaps these electrons were driven down magnetic field lines by resonant electromagnetic-wave interactions that decreased the electron pitch angles.⁵³

Large fluctuations in electron intensities as functions of time and position have been observed in the outer radiation belt.³¹ Louis A. Frank⁵⁴ observed electrons that diffuse inward at the rate of $0.4~r_{\rm e}/{\rm day}$ at L=4.7 decreasing to $0.03~r_{\rm e}/{\rm day}$ at $L=3.4~(r_{\rm e}$ is the radius of the earth). In this L region the diffusion rate was proportional to L^8 . Flux changes have been correlated with magnetic storms.⁵⁵

Are the electrons lost from the magnetosphere into the atmosphere? Or do they change position in the magnetosphere and then return to their original positions? Are the electrons accelerated to higher energies only to relax back to their initial energies? What is the electron loss rate out of the magnetosphere?

Where the electron lifetime is long, only a few of the electrons leak out of the magnetosphere, and a weak source such as CRAND could be responsible for injection. Significant numbers of observed electrons with energies higher than the neutron decay limit of 0.8 MeV could have resulted from diffusion inward while conserving the first adiabatic invariant, satisfying equation 4. Then the observed fluctuations in the outer belt would not be true losses but only temporary changes in the equilibrium distribution.

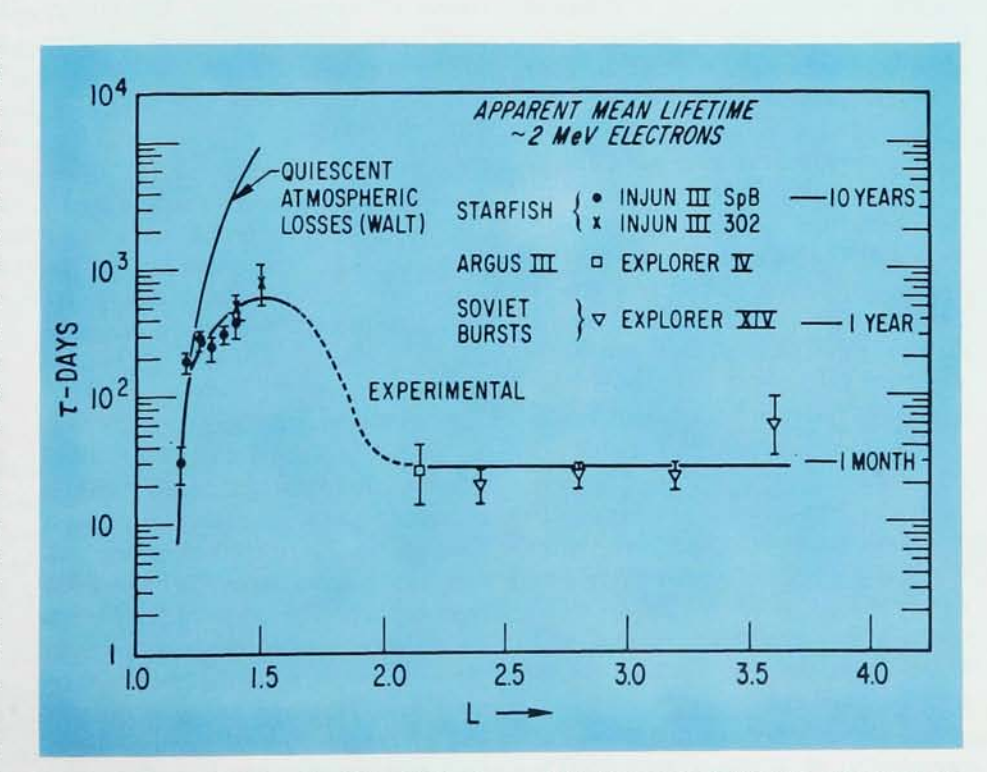
On the other hand, where the lifetime is short, the source must be strong and the only seriously considered contender is the solar wind. The solar wind must furnish electrons that diffuse inward because of magnetic storms. The energy increases with decreasing L according to equation 4. Although diffusion appears to work for low-energy protons (see above "Low-energy protons"), the situation is not so obvious for the electrons, which



LOW-ENERGY PROTONS. Distributions are taken from Mihalov and White,²⁸ 1966. The flux of protons perpendicular to the magnetic field line is plotted versus the proton energy for L=6, 4, 3.5, 3, 2.5, and 2.1, and for B values of 0.1, 0.15, 0.20 and 0.25 gauss. Solid lines are drawn through the data for B=0.10 and 0.25

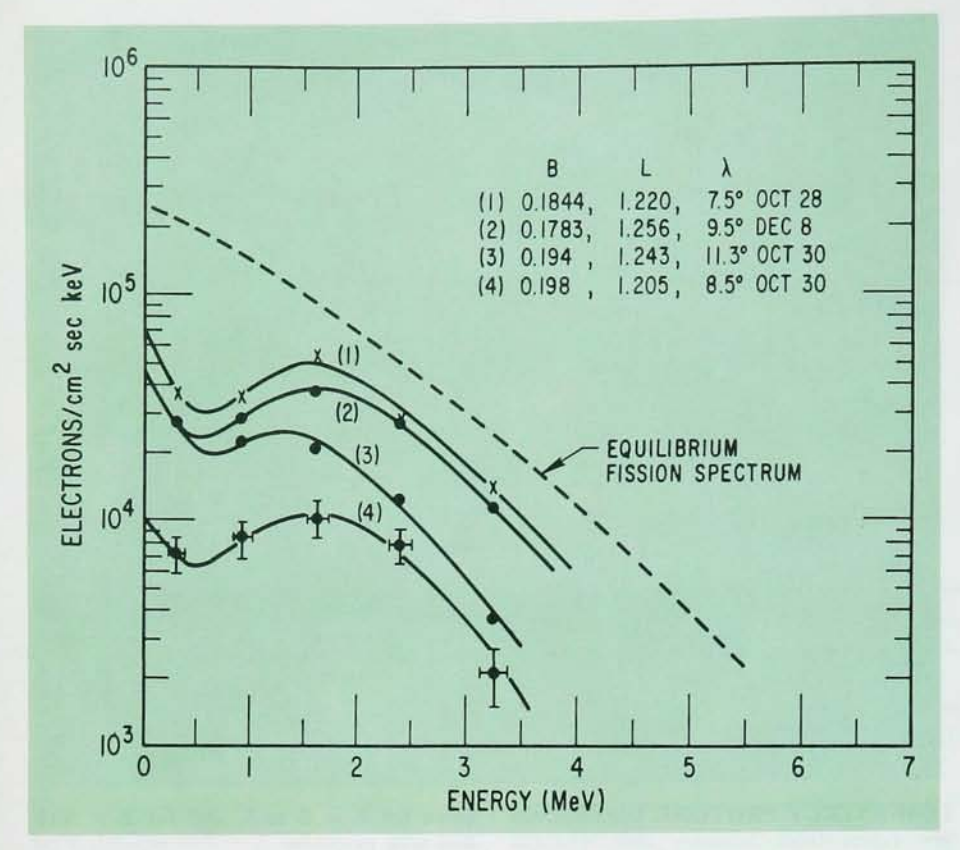
gauss for L=6 to 3, and for B=0.10 and 0.20 gauss for L=2.5 and 2.1. The downward pointing arrow indicates an upper limit. The dashed curves are the theoretical predictions of Nakada and Mead,²⁷ 1965, normalized to the experimental data at L=4 for an energy of 0.25 MeV.

—FIG. 7



LIFETIME VERSUS L MAGNETIC SHELL taken from Van Allen,⁴⁸ 1964. Data points are from Injun 3, Explorers 4

and 14. Theoretical lifetime, computed on the basis of atmospheric losses by Walt,⁴⁹ 1964, is included. -FIG. 8



ELECTRON ENERGY DISTRIBUTION taken from West, Mann and Bloom,⁴⁵ 1965, for measurements in 1962. The solid lines are drawn through the data points

at B, L, and magnetic latitudes listed on the face of the graph. An equilibrium fission spectrum is the dashed line. Data for peak of the Starfish belt. -FIG. 9

do not obey equation 4.56 If diffusion does occur, a source of 100-keV electrons must exist at L=10 at the edge of the magnetosphere. If the solar wind is responsible, the electrons need to be accelerated from the solar wind energy of 1 eV to 100 keV at L=10. Thus, the problem is still not solved, only shifted to finding how and where solar-wind electrons are accelerated. An acceptable alternative is to find a source of 100-keV electrons that can work their way into the magnetosphere. To date no such source has been identified.

Recent detailed electron energy distributions suggest that the Starfishinjected fission electrons are still dominant for L < 1.7. A soft energy distribution appears above the higher-energy fission electrons for L > 1.7 which is in possible agreement with crand injection and with atmospheric scattering and energy loss. 38

The slot is a feature common to all energies, at least above 40 keV. The electron flux increases to a maximum in the outer belt at L=5 and de-

creases at higher L values. The energy distribution gradually becomes softer as L is increased.

Magnetic cavity

The first measurement of the interplanetary magnetic field⁵⁷ with a search coil on Pioneer 5 found an average magnetic field perpendicular to the spacecraft spin axis of 3 gamma (1 gamma = 10^{-5} G). At times of magnetic storms the field fluctuated between 5 and 60 gamma.

More recent experiments on Explorers⁵⁸ 10, 12, 18, and IMP I^{59, 60} have demonstrated clearly that the earth is surrounded by a magnetic cavity that is spherical in the direction of the sun and has a long cometlike tail away from the sun. The shape of the boundary is determined by the interaction of the solar wind with the earth's magnetic field. Its shape has been the subject of considerable theoretical investigation⁶¹ since the configuration derived by J. H. Piddington⁶² to explain geomagnetic storms.

The solar wind was predicted in 1951 by Ludwig F. Biermann⁶³ who needed such a particle flux to explain the deflection of comet tails away from the sun. The solar wind was detected experimentally by A. Bonetti and his coworkers64 with a Faraday Cup on Explorer 10, whose trajectory was in a direction of about 150 deg from the sun-earth direction when it left the tail. On Mariner 2, a good correlation between K_p , an indicator of magnetic activity, and the plasma velocity was found with an electrostatic spectrometer.65 The plasma velocity is given by

$$v \text{ (km/sec)} = 8.44 \Sigma K_p + 330$$
 (6)

14

DE

姐

710

the

地

IW.

Sept 1

34

Mid .

191

11

西山

A further strong 27-day correlation was associated with the rotation of the sun.

Norman F. Ness, Clell S. Scearce and J. B. Seek⁵⁹ used IMP I to map the magnetic field around the earth to distances of 32 earth radii. The boundary of the earth's magnetic field is located at 10 earth radii in the direction of the sun, and at 14 earth radii at 90 deg to the sun-earth direction. Opposite the sun the cavity increases to a cylinder of radius 20 earth radii. This tail continues for a long distance, perhaps several earth-moon distances. The magnetic field is 20 to 30 gamma in the tail. Outside the cavity the plasma energy density dominates. Inside, the magnetic energy is larger.

Ness⁶⁰ discovered a thin neutral sheet in the tail only 600 km thick. The neutral sheet separates the magnetic field in the northern section of the tail, which points toward the earth, from the southern section where the field points away from the earth.

The transition region between the magnetic field boundary and the shock boundary due to the interaction of the plasma with the earth's magnetic field is 3.5 earth radii thick in the sunearth direction and 7 earth radii thick in the perpendicular direction. We summarize with figure 10, which shows the earth's magnetic cavity immersed in the solar wind.

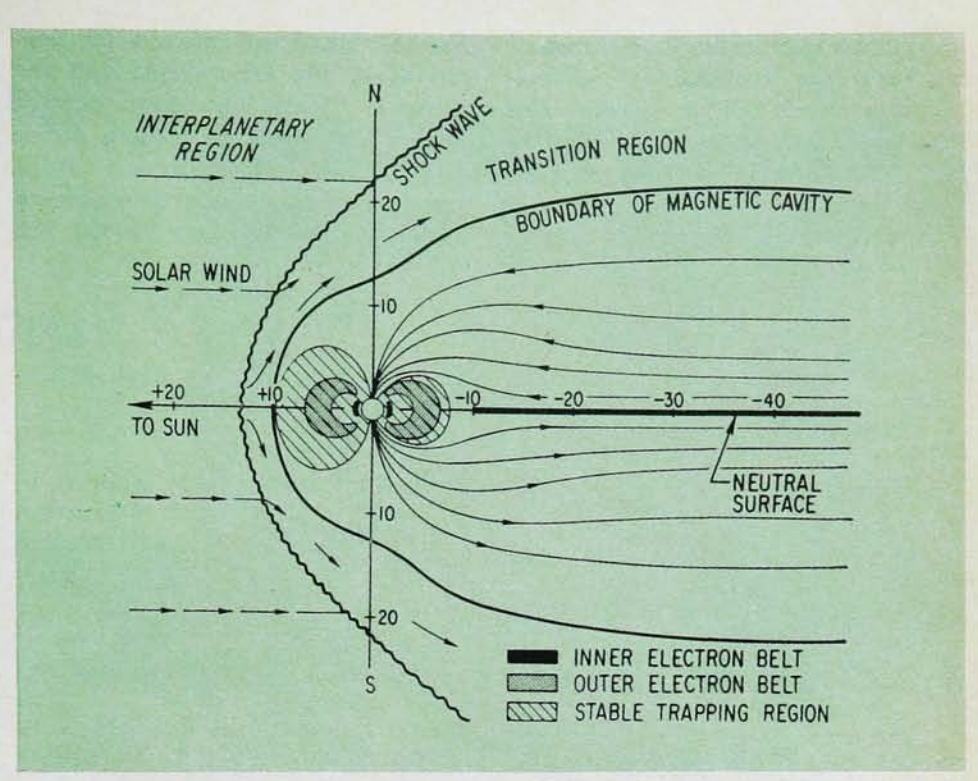
Extensive measurements of the trapped particles near the magnetic field boundary by Frank³² and by John W. Freeman³¹ show that the trapped particles are constrained to 10 earth radii on the sun side of the earth and to about 8 earth radii on the opposite

side. Freeman, from measurements on Explorer 12, reports that electrons with energies greater than 1.6 MeV are peaked at L values of 4 to 5, that electrons more energetic than 40 keV extend out to 10 earth radii in the sun direction but that electrons from 200 to 40 000 eV extend farther out in both directions. The low-energy electrons were those earlier observed with Faraday cups^{33, 34} on Luniks 1 and 2. Electrons with energies greater than 40 keV are sometimes seen in the transition region and in the magnetic tail.66 A drawing of the magnetic cavity is given in figure 11. The inner and outer electron belts are shown in the cutaway. The neutral sheet separates the magnetic field pointing toward the earth in the upper half cylinder from the magnetic field pointing away from the earth in the lower half.

There is speculation that electrons are accelerated in the transition region or in the earth's magnetic tail. The presence of a neutral sheet requires a concentration of charged particles in the sheet. In the model of W. I. Axford, H. E. Petschek and G. L. Siscoe, 67 a potential is set up from one side of the neutral sheet to the other, a distance of 40 earth radii. This potential might be as high as 30 keV. The same potential must then be set up across the polar cap, which supplies the magnetic field lines that are annihilated on the equatorial plane. This potential accelerates electrons from a few electron volts to 30 keV. Alex J. Dessler and R. D. Juday,68 on the other hand, suggest that the auroral electrons are accelerated at the magnetic boundary along the extended tail for a distance of at least 103 earth radii.

Summary

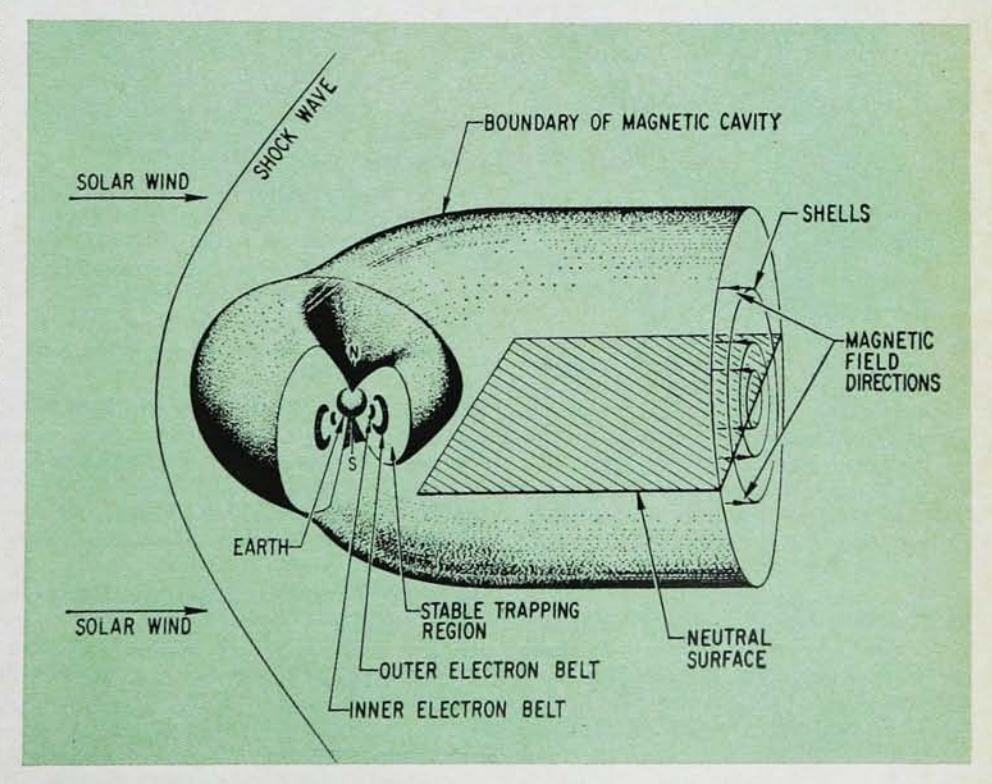
It is useful to summarize the great variety and volume of data that has been accumulated over the last eight years. In one such study, James I. Vette⁶⁹ has compiled a composite trapped innerzone radiation environment. Composite B-L and radius-latitude (R- $\lambda)$ flux maps for electrons with energies greater than 0.5 MeV and for protons with energies greater than 4, 15, 34 and 50 MeV have been prepared. These will be updated from time to time. Flux maps at other energies and at higher L values are currently under preparation. For the



SECTION THROUGH THE MAGNETIC CAVITY given by Ness,60 1965. The shock wave is shown as a wiggly line and the boundary of the magnetic cavity as a solid line with the transition region between. The very heavy line in the direction away from the sun indicates the neutral surface which separates the

magnetic field in the northern halfcylinder of the magnetic tail from that in the southern half. The field lines reverse in crossing the neutral surface. The stable trapping region is indicated with slanted lines, the outer electron belt with dots, and the inner electron belt with a black area.

—FIG. 10



THE MAGNETIC CAVITY. Spherical on the sun side it transforms into a cylindrical tail of radius 20 earth radii opposite the sun. A section shows the earth and the inner and outer electron radiation belts and the region of stable trapping in the sun and antisun direction. The neutral sheet separates the upper half-cylinder where the wind points toward the earth from the lower half-cylinder where it points away from the earth.

—FIG. 11

man-in-space programs it is necessary to know the accumulated radiation doses for specific flight missions. This radiation dose has been computed for a number of typical orbits through the radiation belts.

Throughout this paper an attempt

has been made to emphasize the limitations of the experiments and the theories. These limitations can be further delineated by reading recent comprehensive review articles. Much has been learned about the radiation belts since their discovery in 1958. But

our knowledge is still inadequate to answer the most basic questions. What are the sources and what are the losses of particles in the radiation belts?

This work was performed under Air Force Contracts AF 04(695)569 and AF 04(695)669.

References

- J. A. Van Allen, G. H. Ludwig, E. C. Ray, C. E. McIlwain, Jet Propulsion 28, pp. 588–592 (1958).
- J. A. Van Allen, L. A. Frank, Nature 183, 430 (1959).
- J. A. Van Allen, Scientific American 200, No. 3, 39 (1959).
- 4. S. C. Freden, R. S. White, Phys. Rev. Letters 3, 9 (1959).
- S. C. Freden, R. S. White, J. Geophys. Res. 65, 1377 (1960).
- S. C. Freden, R. S. White, J. Geophys. Res. 67, 25 (1962); H. H. Heckman, A. H. Armstrong, J. Geophys. Res. 67, 1255 (1962).
- S. F. Singer, Phys. Rev. Letters 1, 181 (1958).
- A. J. Dragt, M. M. Austin, R. S. White, J. Geophys. Res. 71, 1293 (1966).
- J. M. Cornwall, A. R. Sims, R. S. White, J. Geophys. Res. 70, 3099 (1965).
- W. N. Hess, Phys. Rev. Letters 3, 11 (1959).
- C. Y. Fan, P. Meyer, J. A. Simpson, J. Geophys. Res. 66, 2607 (1961).
- S. F. Singer, Phys. Rev. Letters 3, 188 (1959).
- 13. A. J. Dragt, J. Geophys. Res. 66, 1641 (1961).
- J. E. Naugle, D. A. Kniffen, J. Geophys. Res. 68, 4065 (1963).
- A. M. Lenchek, J. Geophys. Res. 67, 2145 (1962).
- 16. C. E. McIlwain, Science 142, 355 (1963).
- 17. R. W. Fillius, C. E. McIlwain, Phys. Rev. Letters 12, 609 (1964).
- S. C. Freden, J. B. Blake, G. A. Paulikas, J. Geophys. Res. 70, 3111 (1965).
- C. E. McIlwain, J. Geophys. Res. 66, 3681 (1961).
- 20. T. G. Northrup, E. Teller, Phys. Rev. 117, 215 (1960).
- R. C. Filz, E. Holeman, J. Geophys. Res. 70, 5807 (1965); Harry H. Heckman and George H. Nakano in Space Research V (North-Holland, Amsterdam, 1964), pp. 329–342.
- 22. Leo R. Davis, James M. Williamson in *Space Research III* (North-Holland, Amsterdam, 1963), pp. 365–375.
- 23. S. J. Bame, J. P. Conner, H. H. Hill, F. E. Holly, J. Geophys. Res. **68**, 55 (1963).
- 24. P. J. Kellogg, Nature 183, 1295 (1959).
- E. N. Parker, J. Geophys. Res. 65, 3117 (1960).
- J. W. Dungey, W. N. Hess, M. P. Nakada in Space Research IV (North-Holland, Amsterdam, 1965), pp. 399– 403.

- M. P. Nakada, G. D. Mead, J. Geophys. Res. 70, 4777 (1965).
- J. D. Mihalov, R. S. White, J. Geophys. Res. 71, 2207 (1966).
- B. J. O'Brien, J. A. Van Allen, C. D. Laughlin, L. A. Frank, J. Geophys. Res. 67, 397 (1962).
- 30. L. A. Frank, J. A. Van Allen, H. K. Hills, J. Geophys. Res. 69, 2171 (1964).
- 31. J. W. Freeman, J. Geophys. Res. 69, 1961 (1964).
- L. A. Frank, J. Geophys. Res. 70, 1593 (1965).
- K. I. Gringauz, V. V. Bezrukikh, V. D. Ozerov, R. E. Kybchinskii, Dokl. Akad. Nauk SSSR 131 (6), 1301 (1960).
- K. I. Gringauz, V. G. Kurt, V. I. Moroz, I. S. Shklovskii, Dokl. Akad. Nauk SSSR 132 (5), 1062 (1960).
- 35. S. N. Vernov, A. E. Chudakov, P. V. Valsulov, Yu. I. Logachev, A. G. Nikolayev in *Space Research I* (North-Holland, Amsterdam, 1960), pp. 845–851. (Originally published in Dokl. Akad. Nauk SSSR 130, 517 (1960).)
- F. E. Holly, L. Allen, R. G. Johnson,
 J. Geophys. Res. 66, 1627 (1961).
- J. B. Cladis, L. F. Chase Jr, W. L. Imhof, D. J. Knecht, J. Geophys. Res. 66, 2297 (1961).
- W. N. Hess, J. Geophys. Res. 65, 3107 (1960); W. N. Hess, J. Killeen, J. Geophys. Res. 66, 3671 (1961); W. N. Hess, E. H. Ganfield, R. E. Lingenfelter, J. Geophys. Res. 66, 665 (1961).
- W. N. Hess, J. Killeen, C. Y. Fan, P. Meyer, J. A. Simpson, J. Geophys. Res. 66, 2313 (1961).
- 40. B. J. O'Brien, J. Geophys. Res. 67, 1227 (1962).
- 41. J. R. Burrows and I. B. McDiarmid, Can. J. Phys. 42, 1529 (1964).
- J. D. Mihalov, F. S. Mozer, R. S. White, J. Geophys. Res. 69, 4003 (1964).
- N. C. Christofilos, J. Geophys. Res. 64, 869 (1959).
- J. A. Van Allen, C. E. McIlwain, G. H. Ludwig, J. Geophys. Res. 64, 877 (1959).
- 45. H. I. West Jr, L. G. Mann, S. D. Bloom in *Space Research V* (North-Holland, Amsterdam, 1965), p. 423.
- W. L. Brown, J. D. Gabbe, J. Geophys. Res. 68, 607 (1963).
- C. O. Bostrom, D. J. Williams, J. Geophys. Res. 70, 240 (1965).
- 48. J. A. Van Allen, Nature 203, 1006 (1964).

- M. Walt, J. Geophys. Res. 69, 3947 (1964).
- W. L. Imhof, R. V. Smith, Phys. Rev. Letters 14, 885 (1965).
- 51. J. B. Cladis, Proceedings of advanced study institute on radiation belts held in Bergen, Norway, 16 Aug. to 3 Sept. 1965. To be published by D. Reidel Publishing Company (Dordrecht, Holland).
- G. A. Paulikas, S. C. Freden, J. Geophys. Res. 69, 1239 (1964).
- J. M. Cornwall, J. Geophys. Res. 69, 1251 (1964); J. W. Dungey, Planetary Space Sci. 11, 591 (1963).
- L. A. Frank, J. Geophys. Res. 70, 3533 (1965).
- S. E. Forbush, G. Pizzella, D. Venkatesan, J. Geophys. Res. 67, 3651 (1962).
- J. D. Mihalov, R. S. White, J. Geophys. Res. 71, 2217 (1966).
- 57. P. J. Coleman, L. Davis Jr, C. D. Sonett, Phys. Rev. Letters 5, 43 (1960).
- 58. J. P. Heppner, N. F. Ness, C. S. Scearce, T. L. Skillman, J. Geophys. Res. 68, 1 (1963); L. J. Cahill and P. G. Amazeen, J. Geophys. Res. 68, 1835 (1963).
- N. F. Ness, C. S. Scearce, J. B. Seek,
 J. Geophys. Res. 69, 3531 (1964).
- N. F. Ness, J. Geophys. Res. 70, 2984 (1965).
- W. I. Axford, C. D. Hines, Can. J. Phys. 39, 1433 (1961); J. W. Dungey, Phys. Rev. Letters 6, 47 (1961); J. R. Spreiter, W. P. Jones, J. Geophys. Res. 68, 3555 (1963).
- 62. J. H. Piddington, J. Geophys. Res. 65, 93 (1960).
- 63. L. Biermann, Z. Astrophys. 29, 274 (1951).
- A. Bonetti, H. S. Bridge, A. J. Lazarus,
 B. Rossi, F. Scherb, J. Geophys. Res.
 4017 (1963).

14

91

- C. W. Snyder, M. Neugebauer, V. R. Rao, J. Geophys. Res. 68, 6361 (1963).
- K. A. Anderson, H. K. Harris, R. J. Paoli, J. Geophys. Res. 70, 1039 (1965).
- W. I. Axford, H. E. Petschek, G. L. Siscoe, J. Geophys. Res. 70, 1231 (1965).
- A. J. Dessler, R. D. Juday, Planetary Space Sci. 13, 63 (1965).
- 69. James I. Vette, Models of the Trapped Radiation Environment. Vol. I, Inner zone protons and electrons (National Aeronautics and Space Administration, Washington, 1966) Report No. NASA SP-3024.
- W. N. Hess, G. D. Mead, M. P. Nakada, Rev. Geophys. 3, 521 (1965);
 N. F. Ness, Science 151, 1041 (1966).